The resveratrol analog HS-1793 enhances radiosensitivity of mouse-derived breast cancer cells under hypoxic conditions

YOO JIN CHOI[1], KYU HEO[1], HEE SUNG PARK[1], KWANG MO YANG[1] and MIN HO JEONG[2]

[1]Department of Research Center, Dong Nam Institute of Radiological and Medical Sciences, Busan 619-953; [2]Department of Microbiology, Dong-A University College of Medicine, Busan 602-714, Republic of Korea

Received May 17, 2016; Accepted July 14, 2016

DOI: 10.3892/ijo.2016.3647

Abstract. Tumor hypoxia is associated with treatment resistance, cell proliferation, and metastatic potential, all of which contribute to a poor prognosis. Resveratrol [RES (*trans*-3,4',5-trihydroxystilbene)], a naturally occurring polyphenol, is enriched in grapes and red wine. This study investigated whether the resveratrol analog HS-1793 modulates the hypoxic status and the level of perfusion in mouse breast cancer FM3A cells. Our data show that HS-1793 decreased the levels of hypoxia-inducible factor-1α (HIF-1α) and vascular endothelial growth factor protein under hypoxic conditions in FM3A cells. HS-1793 improved perfusion and hypoxic status in tumor tissues and inhibited angiogenesis through HIF-1α suppression in mice. Moreover, HS-1793 inhibited hypoxia-induced cancer stem cell properties and enhanced ionizing radiation-induced apoptosis in hypoxic FM3A cells. Collectively, the resveratrol analog HS-1793 might act as a potent radiosensitizer and be a useful adjuvant agent against radiotherapy-resistant hypoxic cells in solid tumors.

Introduction

Hypoxia is a reduction in the normal level of tissue oxygen tension and occurs in many disease processes, including cancer. Tumor hypoxia is typically associated with poor patient prognosis, partly because low oxygen levels reduce the effectiveness of radiation therapy, which kills tumor cells by generating reactive oxygen species (1). Hypoxia-inducible factor (HIF) is a transcription factor found in mammalian cells cultured under reduced oxygen tension and plays a key role in the cellular response to hypoxia. HIF regulates the transcription of several genes involved in biological processes, such as angiogenesis, cell proliferation and survival, glucose metabolism, pH regulation and apoptosis (2). Angiogenesis is a crucial regulator of tumor growth and metastases (3). Tumor angiogenesis is regulated by the production of angiogenic stimulators, including vascular endothelial growth factor (VEGF), which is a key regulatory factor in the prognosis of various cancers. Several studies have shown that transforming growth factor-β1 (TGF-β1) is involved in angiogenesis, leading to tumor progression (4). TGF-β1 signaling has been shown in concert with HIF-1α to regulate VEGFA expression (5).

Cancer stem cells (CSCs) typically represent a small fraction of tumor cells that have the ability to self-renew and differentiate into many more mature cancer cells (6). HIF stabilization in hypoxic tumor cells may promote the adoption of stem cell properties, including self-renewal and multipotency, by stimulating the expression or activity of Oct4, Notch, and other critical signaling pathways. Oct4 has been shown to function in a complex with Nanog and Sox2 to activate and repress genes controlling stem cell identity and differentiation (7). KLF4 is highly expressed in CSC-enriched populations in mouse primary mammary tumors and breast cancer cell lines (8). Indeed, CSCs have been shown to be more radioresistant than non-stem cancer cells and are, therefore, believed to be responsible for treatment failure and tumor recurrence (9).

Among females, breast cancer ranks first at age 20-59 years (10). In recent years, the encouraging trend towards earlier detection and the increasing use of systemic adjuvant treatment have improved survival rates; however, nearly half of the breast cancer patients treated for localized disease develop metastasis (11). A lower incidence of breast cancer is associated with the high consumption of phytoestrogens, which are biologically active plant-derived phenolic compounds that structurally mimic the mammalian estrogen 17β-estradiol (12). Basic and preclinical research have focused on resveratrol [RES (*trans*-3,4',5-trihydroxystilbene)], a naturally occurring polyphenol enriched in grapes and red wine (13). Resveratrol has recently been shown to function as a cancer chemoprevention agent, an anti-mutagenic agent, and an anti-initiative agent (14).

This study demonstrated that the resveratrol analog HS-1793 inhibits angiogenesis via the regulation of hypoxia and displays hypoxia-induced CSC properties in FM3A mouse breast cancer cells.

Correspondence to: Dr Kwang Mo Yang, Department of Research Center, Dong Nam Institute of Radiological and Medical Sciences, Busan 619-953, Republic of Korea
E-mail: kmyang@dirams.re.kr

Dr Min Ho Jeong, Department of Microbiology, College of Medicine, Dong-A University, Busan 602-714, Republic of Korea
E-mail: mhjeong@dau.ac.kr

Key words: resveratrol, HS-1793, hypoxia, cancer stem cell, radiation

Materials and methods

Preparation of HS-1793. To obtain HS-1793, the stilbene double bond present in resveratrol was substituted with a naphthalene ring, as previously described (15). A stock solution was generated in absolute ethanol at 50 mM, and the working dilutions were generated directly in culture media. The control vehicle was culture media containing amounts of ethanol equivalent to those present in HS-1793.

Cell culture conditions. FM3A (murine breast cancer cells) originated from the mammary gland of the C3H/He mouse were grown in RPMI-1640 (Gibco, Carlsbad, CA, USA) containing 10% fetal bovine serum (FBS; Hyclone, Logan, UT, USA), 100 U/ml penicillin/streptomycin (Gibco), in a humidified atmosphere containing 5% CO_2 and 37˚C. Exponentially growing cells (~70-80% confluence) in complete medium were pretreated for 2 h with different concentrations of HS-1793, followed by exposure to normoxic (5% CO_2 at 37˚C) or hypoxic conditions (1% O_2 at 37˚C) in an Anaerobic Glove Box (Forma Scientific, Marietta, OH, USA) for treatment. Environmental hypoxic conditions (1% O_2) were achieved in an airtight humidified chamber continuously flushed with a gas mixture containing 5% CO_2 and 95% N_2.

HS-1793 treatment and assessment of cell viability. HS-1793 was dissolved in EtOH and stored at -80˚C until use. FM3A cells were plated onto 60-mm dishes with $1x10^5$ cells for 24 h, and the cells were treated with HS-1793 (0, 1.3, 2.5, 5, 10 and 20 μM) under normoxic or hypoxic conditions. The cells were harvested at 12 or 24 h after treatment and counted using the ADAM automatic cell counter (Digital Bio., Korea). The relative cell count was determined as follows: final count of treated cultures/final count of control cultures x 100.

Hypoxia detection in tumor cells. To validate the efficiency of hypoxic treatment, a hypoxia detection kit (Hypoxyprobe-1; Chemicon, Temecula, CA, USA) was used to identify 2-nitroimidazole adducts formed in cultured FM3A cells under hypoxia. FM3A cells were cultured on 24-well plates at a density of $1x10^5$ cells/well for 24 h; then, the cells were treated with HS-1793 for 2 h, followed by incubation under normoxic or hypoxic conditions for 12 h. After treatment with 100 μM pimonidazole hydrochloride (1-[(2-hydroxo-3-piperidinyl) propyl]-2-nitroimidazole hydrochloride) under hypoxic conditions for 4 h, single-cell suspensions were prepared with trypsin and spun in clean, fat-free glass slides using a cytocentrifuge. Cytocentrifuged cells were fixed for 30 min in 4% paraformaldehyde (PFA). After washing with phosphate-buffered saline (PBS), the cells were permeabilized with PBS containing 0.5% Triton X-100 for 10 min. Next, the cells were incubated for 30 min at room temperature with FITC-conjugated antibody (1:50) against pimonidazole adducts. Hoechst 33342 was used as a nuclear counterstaining agent. The cells were imaged under Nikon Eclipse TS100 fluorescence microscopy (Nikon, Tokyo, Japan).

Western blot analysis. Protein samples were separated by 10% SDS-PAGE and transferred to a polyvinylidene difluoride membrane. The membrane was allowed to react with anti-HIF-1α (1:200; Novus, USA), anti-VEGF (1:500; Santa Cruz Biotechnology, CA, USA), anti-OCT4 (1:200; Santa Cruz Biotechnology), anti-KLF4 (1:500; Abcam, UK), anti-SOX (1:200; Santa Cruz) or anti-GAPDH (1:2,000; Santa Cruz Biotechnology). Immunostaining with antibodies was performed using the Super-Signal West Pico enhanced chemiluminescence substrate, and detection was performed using LAS-3000PLUS (Fuji Photo Film Co., Kanagawa, Japan).

Cell migration assay. The cells were grown to confluence in 6-well plates for 2 days, and a scrape in the form of a cross was created through the confluent monolayers with a plastic pipette tip. The cells were treated with HS-1793 for 2 h, followed by incubation under normoxic or hypoxic conditions for 24 h. Several wounded areas were marked for orientation, observed, and then imaged using a Nikon Eclipse TS100 microscope (Nikon) at 24 h after the scratch.

Annexin-V binding assay. FM3A cells were pretreated with 2.5 μM HS-1793 for 2 h, followed by incubation under hypoxic conditions. After 12 h, these cells were exposed to γ-IR (0, 2, 4 Gy) using a 137Cs source (BioBeam 8000, STS, Braunschweig, Germany) and cultured under hypoxic conditions for 12 h. The cells were harvested and then washed with PBS. The pellets were resuspended in 1X Annexin V binding buffer (BD Biosciences, Bedford, MA, USA) at a concentration of $1x10^6$ cells/ml. Next, 100 μl of the solution was transferred to a 5-ml culture tube, and 5 μl of Annexin V-FITC and 5 μl 7-AAD were added. The cells were then gently vortexed and incubated for 15 min at RT (25˚C) in the dark. Next, 400 μl of 1X binding buffer was added to each tube, and the samples were analyzed by flow cytometry (BD FACSAria, USA) within 1 h.

Animal studies. All experiments were performed on 6-week-old C3H/He female mice obtained from Central Lab. Animal Inc. (Seoul, Korea). The animals were raised under SPF conditions at the Korea Institute of Toxicology, Hospital of Dong-A University according to Good Laboratory Practices OECD guidelines. All animal procedures were performed according to approved protocols (approval no. DIACUC-09-24) from the Institutional Animal Care and Use Committee (IACUC) of Dong-A University and in accordance with recommendations for the proper use and care of laboratory animals. FM3A cells in logarithmic growth phase were used to establish a breast tumor model. Xenografts were generated by subcutaneously injecting $2x10^6$ tumor cells in 50 μl of PBS into the flank adjacent to the right hind limb of 7-week-old female C3H/He mice. When the tumor grew to a size of ~500 mm^3, HS-1793 (1.5 mg/kg) was administered as an intraperitoneal (i.p.) single injection for the determination of the hypoxic status and perfusion level in the tumor tissue. When the tumor grew to a size of ~40 mm^3 (~10 days), the mice were stratified into groups of 8-10 animals with equal mean tumor volumes, and HS-1793 (0.1, 0.5 and 1.5 mg/kg) was administered by i.p. injection twice a week for 30 days. The tumor sizes were measured with calipers once weekly. The tumor volume was calculated as follows: $(width)^2$ x length x 0.52. After 4 weeks, the mice were euthanized to obtain serum samples and tumor tissues.

ELISA. The serum VEGF concentrations from animals bearing xenografts were determined. The blood was collected from the abdominal vein of tumor-bearing or normal mice at 40 days after the inoculation of tumor cells. Serum samples were obtained by centrifugation at 3,000 rpm for 10 min and stored at -20˚C until further analysis. The VEGF concentrations were determined using a quantitative enzyme-linked immunosorbent assay (ELISA, R&D Systems, Minneapolis, MN, USA). The amount of VEGF immunoreactivity was calculated using recombinant mouse VEGF standards present on each microtiter plate. Optical densities were determined at 550 nm using a microtiter plate spectrophotometer (Beckman Coulter detection platform, USA).

Real-time PCR quantification. Total cellular RNA was isolated from tumor tissue using TRIzol reagent (Invitrogen) and used for reverse transcription. Complementary DNA (cDNA) was synthesized from 1 μg of total RNA from each sample using a Maxime RT PreMix (iNtRON) according to the manufacturer's instructions and used as a template for TaqMan™ real-time quantitative PCR. The relative mRNA levels were quantified using fluorescent TaqMan® technology. PCR primers and probes specific for murine VEGF (assay ID: mM 01281449_m1) and HIF-1α (assay ID: mM 00468869_m1) were obtained as TaqMan Gene Expression arrays (Applied Biosystems, Germany). Glyceraldehyde-3-A phosphate-dehydrogenase (GAPDH) (assay ID: mM 99999915_g1) was used as an internal control. PCR amplifications of HIF-1α, VEGF and GADPH were performed in 20-μl volumes and in separate reactions. The mix contained 1 μl of the 20X ready-to-use primer and probe mix for HIF-1α, VEGF or GAPDH, 2 μl of the undiluted cDNA, and 10 μl of the 2X TaqMan Universal Master Mix (Applied Biosystems). The probe was labeled at the 5'-end with the reporter molecule 6-carboxy-fluorescein (FMA) and at the 3'-end with a non-fluorescent quencher and MGB. PCR assays were performed using a CFX96 Real-Time PCR Detection system (Bio-Rad, Mississauga, ON, Canada). The PCR was initiated with a 2-min incubation at 50˚C and then an initial 10-min denaturation at 95˚C, followed by a total of 50 cycles of 15-sec denaturation at 95˚C, and 1 min of annealing and elongation at 60˚C. For each sample, ΔΔCt (crossing point) values were calculated as the Ct of the target gene minus the Ct of the GAPDH gene. Gene expression was derived according to the $2^{-\Delta\Delta Ct}$ method; changes in gene expression are expressed relative to the basal condition.

Determination of the hypoxic status and perfusion level in tumor tissue. As markers of hypoxia, pimonidazole hydrochloride (1-[(2-hydroxo-3-piperidinyl)propyl]-2-nitroimidazole hydrochloride) (16,17) and CCI-103F (1-(2-hydroxy-3-hexafluoroisopropoxy-propyl)-2-nitroimidazole) (18) were used. Pimonidazole hydrochloride (Hypoxyprobe-1 Plus kit; Chemicon) and CCI-103F (Hypoxyprobe F6 kit; Chemicon) are bioreductive chemical probes with an immunorecognizable side chain. The addition of the first electron in the bioreductive activation is reversibly inhibited by oxygen, resulting in futile cycling with a half maximal pO_2 of inhibition of ~3 mM Hg and with complete inhibition occurring at ~10 mM Hg (17). Pimonidazole hydrochloride was dissolved in saline, and CCI-103F was dissolved in 10% dimethyl sulfoxide (DMSO) and 90% peanut oil. To determine the effect of HS-1793 on vessel functionality, the double-fluorescent dye technique based on the perfusion markers, Hoechst 33342 (Sigma-Aldrich) and DiOC7 (Invitrogen) were used. Hoechst 33342 and DiOC7 are removed very rapidly from the circulation (half-time of 2 min) and are very stable once bound to DNA. Thus, Hoechst 33342 and DiOC7 specifically label the nuclei and mitochondria of endothelial cells, respectively, and those of the cells adjacent to the vessel walls, thereby delineating the perfused vessels (19,20). Hoechst 33342 and DiOC7 were dissolved in saline.

For the single-injection efficacy of HS-1793 concerning the change in tumor hypoxia, pimonidazole (60 mg/kg) was administered for 4 h 15 min, HS-1793 (1.5 mg/kg) was administered for 2 h 15 min, and CCI-103F (60 mg/kg) was administered for 2 h before animal euthanasia (Fig. 2A). With regard to the single-injection efficacy of HS-1793 and the change in tumor perfusion, Hoechst 33342 (15 mg/kg) was administered for 26 min, HS-1793 (1.5 mg/kg) was administered for 16 min, and DiOC7 (1 mg/kg) was administered for 1 min before animal euthanasia (Fig. 2B). For the 30-day repeat injection efficacy of HS-1793 (0.5, 1 and 1.5 mg/kg), pimonidazole hydrochloride was injected intravenously (i.v.) into the tail vein at a dose of 60 mg/kg, and Hoechst 33342 was injected i.v. at a dose of 15 mg/kg in a total volume of 0.1 ml. Pimonidazole hydrochloride was administered for 2 h, and H33342 was administered for 1 min before animal euthanasia. After animal euthanasia, the tumor specimens were removed and frozen in OCT mounting medium (Sakura Finetek, Torrance, CA, USA). Next, consecutive 4-μm-thick frozen sections were cut on a Shandon Cryotome FSE (Thermo Fisher, Waltham, MA, USA). The sections were then stored at -80˚C until staining.

IHC staining and fluorescence microscopy in tumor tissues. After thawing, the sections were fixed in cold acetone (4˚C) for 30 min. Between all consecutive steps of the staining procedure, the sections were rinsed once for 5 min in 1X Tris-buffered saline with 0.1% Tween-20 (TBS-T). Unless otherwise stated, all antibodies were diluted in PBS with 1% bovine serum albumin (BSA). The sections on slides were treated with rabbit anti-CD31 polyclonal antibody (1:100; Abcam, ab28364) or mouse anti-HIF-1α polyclonal antibody (1:100; Abcam, ab1) as a primary antibody overnight at 4˚C. The sections were washed and then treated with a secondary antibody using the Envision Detection kit (Dako, K5007). Pimonidazole and CCI-103F are reductively activated in hypoxic cells and forms stable adducts with thiol groups in proteins, peptides, and amino acids. FITC-MAb1 (fluorescein-conjugated mouse IgG1 monoclonal antibody clone) and rabbit anti-CCI-103F antisera (PAbF6) bind to these adducts, allowing their detection by immunochemical means. The tumor sections were rehydrated and preincubated for 15 min with 1% BSA, immediately followed by incubation with FITC-conjugated anti-pimonidazole antibody (1:50) for 30 min and rabbit anti-CCI-103F antisera (PAbF6) (1:50) for 1 h at room temperature, respectively. For CCI-103F staining, the sections were washed and then treated with Texas Red Anti-Rabbit IgG (Vector, TI-100) (1:100) for 1 h at room temperature. Finally, the tumor sections were mounted with Malinol (Muto Pure Co.) and covered with a cover slip. The tumor sections were stored at 4˚C and scanned within 1-2 days after staining.

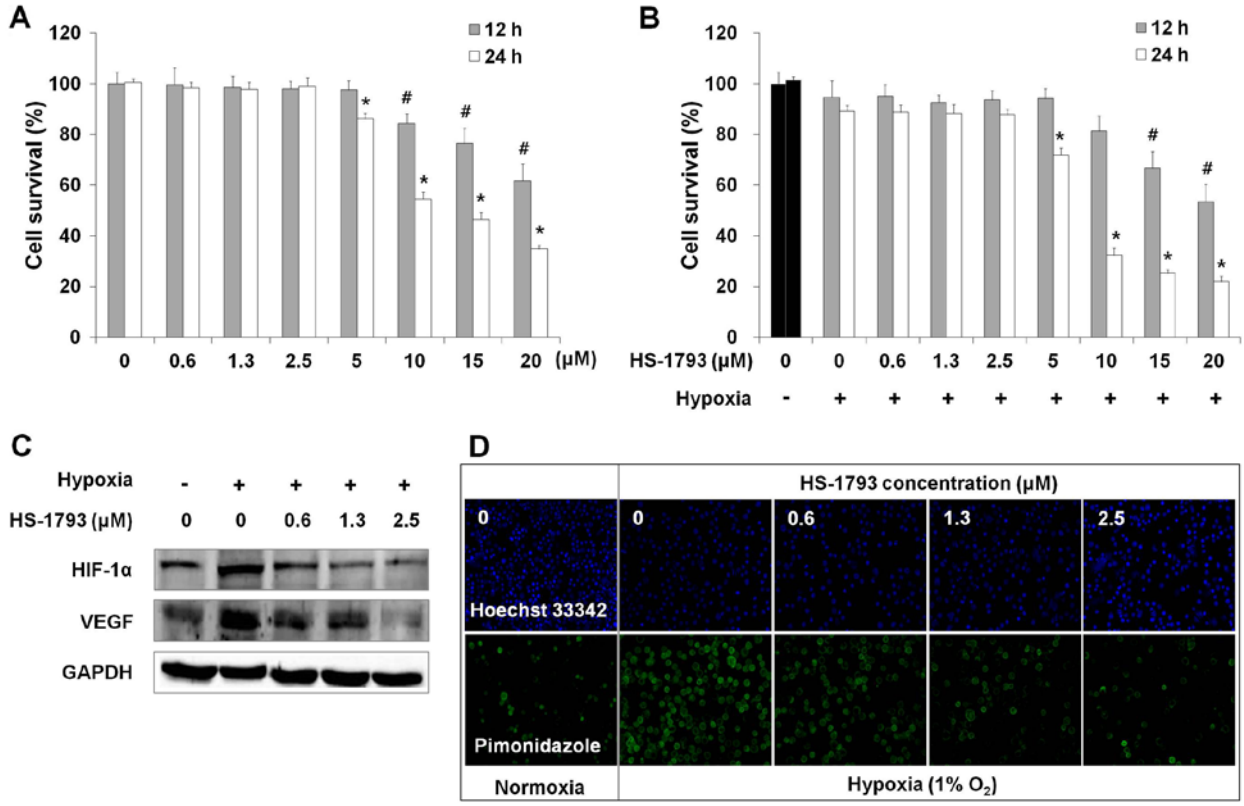

Figure 1. Effect of HS-1793 on the change in the hypoxic condition in FM3A cells. The cells were treated with different concentrations of HS-1793 for 2 h. Next, the cells were cultured under normoxic (A) or hypoxic (B) conditions for 12 or 24 h. Cell viability was determined after the treatment time and is expressed as a percentage of control growing cells. The cell lysates were subjected to immunoblot analysis with anti-HIF-1α and anti-VEGF (C). After HS-1793 treatment, the cells were incubated in the presence of 100 μM pimonidazol hydrochloride for 4 h and were fixed with 4% PFA. The cells were incubated for 30 min at room temperature with FITC-conjugated anti-pimonidazole antibody, and Hoechst 33342 was used as a nuclear counterstaining agent. The cells were imaged under Nikon Eclipse TS100 fluorescence microscopy (x200) (D). The data are expressed as the mean ± SD, and significant differences emerged between the treated groups by ANOVA followed by Dunnett's test. *P<0.05 compared with the untreated control (0 μM) for the 24-h condition and $^{\#}$P<0.05 compared with untreated control (0 μM) for the 12-h condition.

The different fluorescence excitation and emission properties of the Hoechst 33342 and DiOC7 dyes allow for the detection of temporal and spatial fluctuations in perfusion. Examinations were performed under a Nikon Eclipse 80i microscope (Nikon) equipped with Image Pro Plus 7.0 software (Media Cybernetics, Silver Spring, MD, USA).

Analysis of hypoxia and the perfused vasculature. The tumor sections were quantitatively analyzed using a semiautomatic method based on a computerized digital image analysis system. A high-resolution intensified solid-state camera on a fluorescence microscope (Nikon Eclipse 80i, Japan) with a computer-controlled motorized stepping stage was used. Each tumor cross-section was sequentially scanned at x40 magnification using different filters for the Hoechst 33342 (blue), FITC (green), and Texas Red signals. After each scan, one composite digital image was reconstructed from the individual microscopic fields. The entire scanning procedure thus yielded three composite images from each tumor section that was analyzed with Image Pro Plus 7.0 software (Media Cybernetics). The figures were prepared using Adobe Photoshop 7.0. depending on the structures and markers visualized, different composite images were obtained. For the qualitative analysis of changes caused by oxygen-modifying intervention, both hypoxic and perfusion markers were stained on the same tissue. This process resulted in composite binary images showing the hypoxic markers CCI-103F (Texas Red) and pimonidazole (FITC) and the perfusion markers Hoechst 33342 (blue) and DiOC7 (green). We quantified the staining in two ways: the thresholds were applied to the pimonidazole and CCI-103F images to derive the fractions of the tumor section that were positive for each marker. Threshold values are inevitably arbitrary and subject to the possibility that a different threshold value would yield different results. To investigate this possibility, we exported the image histograms into Excel and generated positive fractions for each threshold value.

Statistical analysis. The results are expressed as the mean ± standard deviation (SD). Significant differences between the treatments and control were evaluated by ANOVA (Dunnett's test). A P-value <0.05 was defined as statistically significant.

Results

HS-1793 changes the hypoxic condition in FM3A cells. To detect the cytotoxicity of HS-1793 in FM3A cells, we treated the cells with different concentrations of HS-1793 for 12 or 24 h under normoxic or hypoxic conditions, and we then measured the viability of FM3A cells. In Fig. 1A and B, no marked reduction of cell viability ≤2.5 μM HS-1793 was

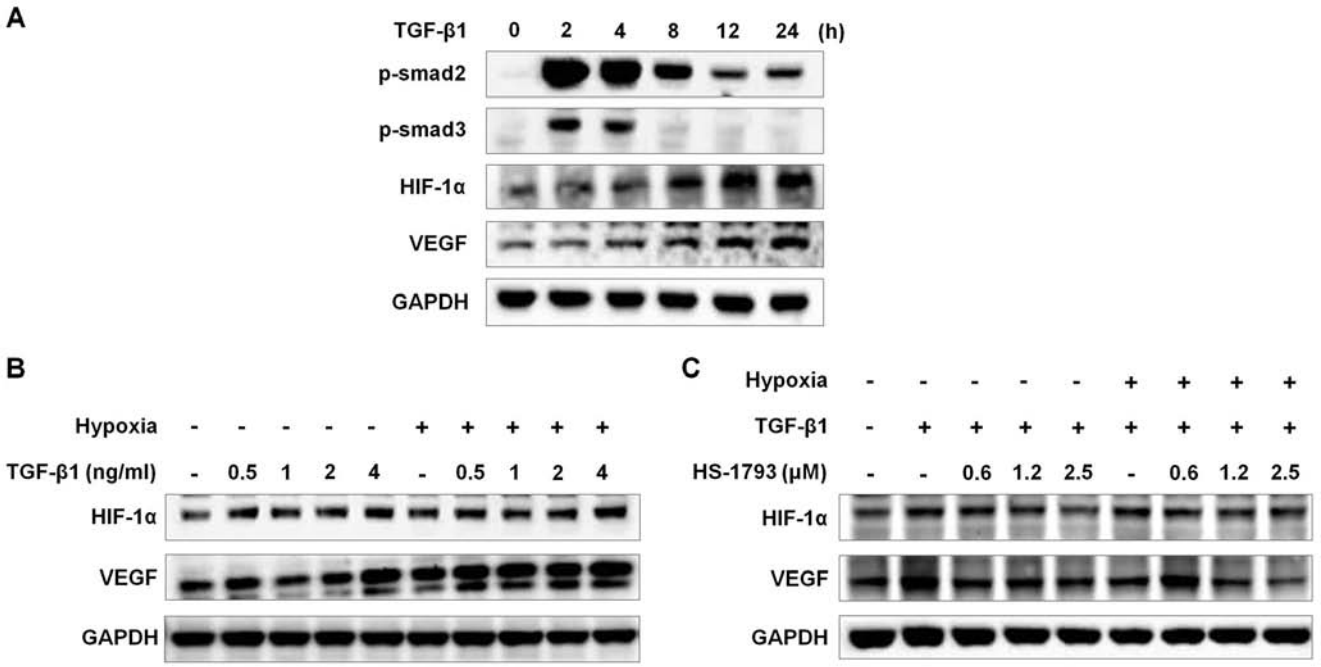

Figure 2. Effect of HS-1793 on TGF-β1 induced HIF-1α and VEGF expression in FM3A cells. The cells were treated with TGF-β1 (4 ng/ml) for the indicated times, and the HIF-1α, VEGF and phosphorylated forms of Smads (p-Smads) were detected by immunoblot assay (A). Dose-dependent induction of HIF-1α and VEGF expression by TGF-β1 under normoxic or hypoxic conditions (B). The cells were treated with different concentrations of HS-1793 for 2 h. Next, the cells were treated with TGF-β1 (4 ng/ml) under normoxic or hypoxic conditions for 12 h. The cell lysates were subjected to immunoblot analysis (C).

observed under either normoxic or hypoxic conditions in FM3A cells at 12 or 24 h. Thus, we used 0.6, 1.3 and 2.5 μM HS-1793 in subsequent experiments. We explored whether HS-1793 inhibits HIF-1α and VEGF expression relative to angiogenesis under hypoxic conditions of the tumor microenvironment. Pretreatment of FM3A cells with HS-1793 resulted in a dose-dependent decrease in hypoxia-induced HIF-1α and VEGF protein levels (Fig. 1C).

To investigate whether HS-1793 regulates the hypoxic tumor microenvironment, we evaluated FM3A cells under hypoxic conditions. The cells were treated with HS-1793 under hypoxic conditions for 12 h and added characteristic pimonidazole adducts of hypoxia. In Fig. 1D, the fluorescent expression of pimonidazole was increased under hypoxic conditions compared with that under normoxic conditions. However, HS-1793 reduced the fluorescent expression of pimonidazole dose-dependently.

HS-1793 reduces TGF-β1-induced HIF-1α accumulation and VEGF expression in FM3A cells. HIF-1α plays a crucial role in VEGF induction under hypoxic conditions. To explore the role of TGF-β1 in HIF-1α and VEGF expression under normoxic conditions, we initially evaluated the effect of TGF-β1 on HIF-1α and VEGF expression in FM3A cells. HIF-1α and VEGF expression was upregulated by TGF-β1 at the protein level in a time-dependent manner. An increase in the HIF-1α level was clearly detectable 12 h after treatment, indicating that TGF-β1 enhances the stability of HIF-1α proteins in FM3A cells. To explore the signaling pathways implicated in the TGF-β1 induction of VEGF, we investigated the involvement of the Smad pathway, a crucial mediator of the TGF-β1 signaling cascade. In response to TGF-β1, the levels of Smad2 and Smad 3 phosphorylation were increased in FM3A cells (Fig. 2A). Moreover, FM3A cells were treated with TGF-β1 under normoxic and hypoxic conditions for 12 h. As shown in Fig. 2B, the HIF-1α and VEGF protein levels were markedly increased by TGF-β1. However, pretreatment with HS-1793 in FM3A cells reduced HIF-1α and VEGF expression dose-dependently (Fig. 2C). Therefore, these findings suggest that HS-1793 inhibits angiogenesis via the regulation of HIF-1α and VEGF expression not only under hypoxia but also under the TGF-β1-treated condition.

HS-1793 improves the perfusion level and hypoxic status in tumor tissues in mice. We assessed blood flow fluctuations in HS-1793-injected mice bearing FM3A breast cancer cells using the double-fluorescent dye method based on two perfusion markers, Hoechst 33342 and DiOC7. Fluorescence microscopy revealed similar intensities to Hoechst 33342 and DiOC7 in control FM3A breast tumors. By contrast, HS-1793-treated (1.5 mg/kg) tumors showed uniform uptake of DiOC7 dye, indicative of improved vessel functionality. To determine whether HS-1793 leads to decreased tumor hypoxia, mice bearing tumors were injected with the hypoxia markers pimonidazole and CCI-103F. Pimonidazole and CCI-103F were stained with green (FITC) and red (Texas Red) colors, respectively, on the photomicrograph. At 2-h time point, the staining intensities of the two hypoxia markers within the same range of a control tumor were similar between pimonidazole and CCI-103F. The extensive hypoxia that was present before HS-1793 treatment (1.5 mg/kg) (hypoxic fraction determined by pimonidazole staining) was reduced after HS-1793 treatment (1.5 mg/kg) (hypoxic fraction determined by CCI-103F staining) (Fig. 3C). As shown in Fig. 3D, a significant differ-

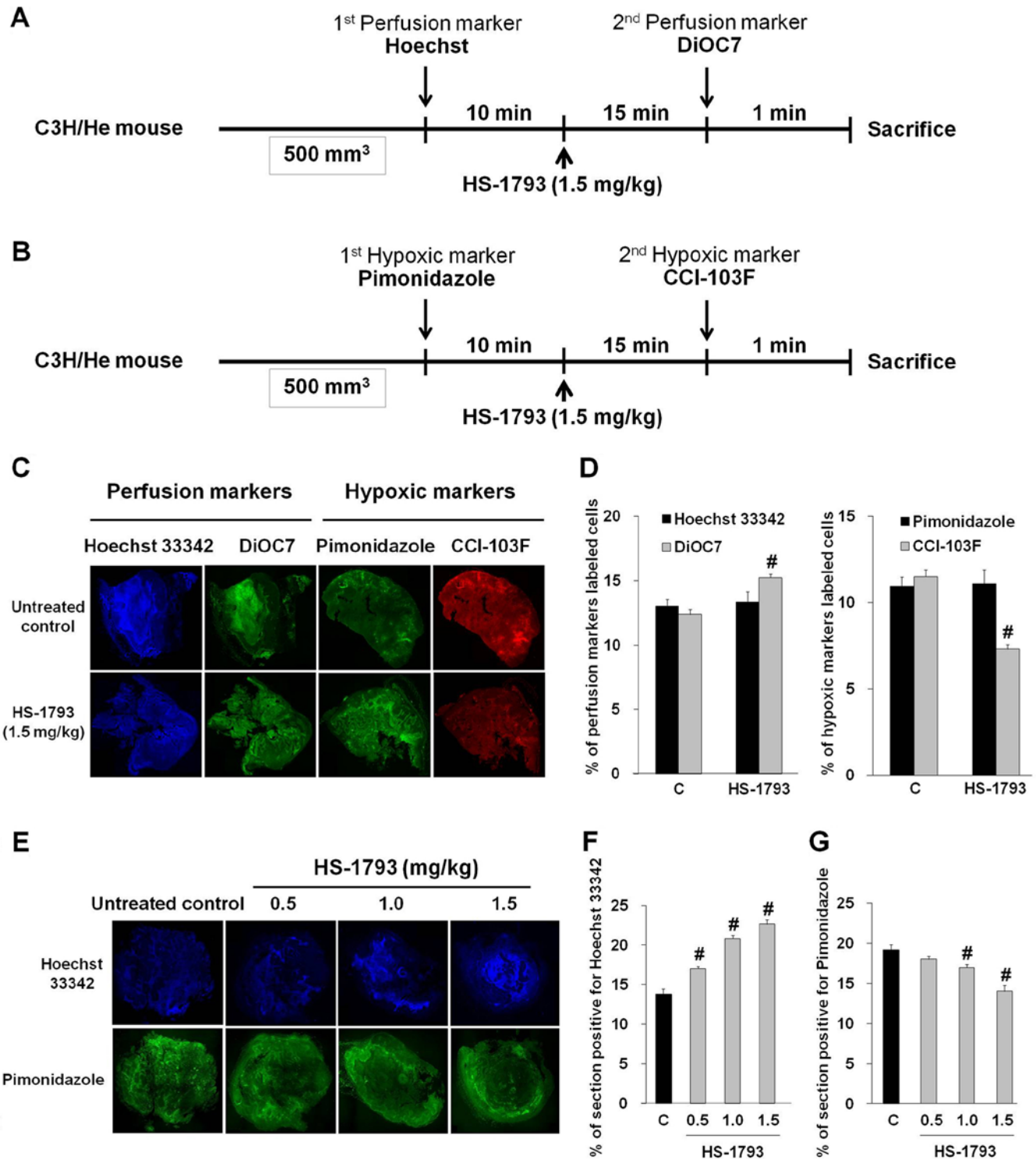

Figure 3. Changes in tumor perfusion and hypoxia after HS-1793 treatment in FM3A tumor-bearing mice. Experimental setup with the injection schedule for the two sequentially administered hypoxic (A) and perfusion cell markers (B). Composite panoramic sections (original x40, reduced for panoramic view) in tumors stained for both perfusion (Hoechst 33342, blue; DiOC7, green) and hypoxia markers (Pimonidazole, green; CCI 103F, red) (C). The mean perfusion and hypoxic fractions were exported as image histograms into Excel, and positive fractions were generated for each threshold value (D). Composite panoramic sections (original x40, reduced for panoramic view) in the tumor tissue (untreated control, 0.5, 1 and 1.5 mg/kg) captured the Hoechst 33342-labeled cells (upper) and pimonidazole-stained cells (down). Tissue regions of a section from a tumor isolated on day 30 (E). The mean Hoechst and pimonidazole fraction were exported as image histograms into Excel, and positive fractions were generated for each threshold value (F and G). #P<0.05, compared with the untreated control.

ence between the untreated and HS-1793-treated images was obtained over a wide range of threshold values.

The mean number of Hoechst 33342-labeled cells represents the blood perfusion of the tumors and indirectly represents the level of hypoxia in the tumors. The lower number of labeled cells suggests impaired blood perfusion and a higher level of hypoxia in the tumors. The Hoechst 33342 stain appeared as a blue color on the photomicrograph (Fig. 3E). The percent-

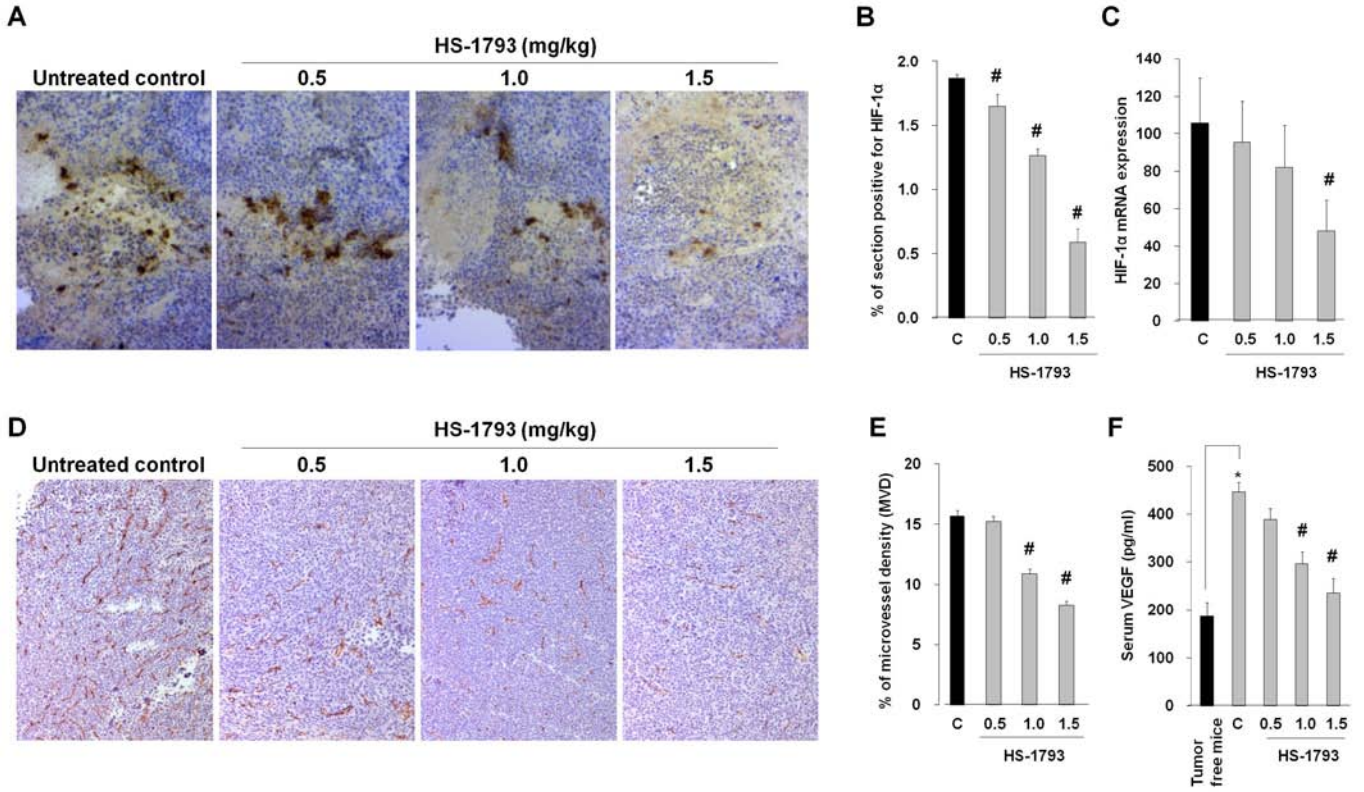

Figure 4. Suppression of HIF-1α expression and anti-angiogenic activity after HS-1793 treatment in FM3A xenografts. C3H/He female mice were inoculated by single s.c. injection of $2x10^6$ FM3A tumor cells in 50 μl of PBS. Mice were treated with HS-1793 (0.5, 1 and 1.5 mg/kg, i.p.) twice a week for 30 days when the tumor grew to a size of ~40 mm^3. Typical microscopic fields of FM3A xenografts immunostained for HIF-1α (A). Quantitative data obtained by immunohistochemical analysis (B). Real-time PCR was performed with specific HIF-1α (C). Typical microscopic fields of FM3A xenografts immunostained for CD31 (D). The microvessel density of FM3A was determined as described above (E). The serum VEGF concentrations from animals bearing xenografts were determined using a quantitative enzyme-linked immunosorbent assay (ELISA, R&D Systems) (F). The data are expressed as the mean ± SD of five mice per group. *P<0.05, compared with tumor-free mice. #P<0.05, compared with the untreated control. Tumor regions of a section from a tumor isolated on day 30. Original magnification, x200.

ages of Hoechst 33342-labeled cells in the untreated control and HS-1793 treated groups (0.5/1.0/1.5 mg/kg) were 13.8 and 17.0/20.9/22.6%, respectively (Fig. 3F). The number of labeled cells in the HS-1793-treated group increased significantly compared with that in the untreated control group. This result suggests increased blood perfusion and slightly decreased tumor hypoxia after HS-1793 treatment.

To examine the effects of HS-1793 treatment on tumor hypoxia, the changes in the extent of the hypoxic areas in FM3A xenografts were assessed by immunohistochemical analysis with pimonidazole. As shown in Fig. 3E, an obvious reduction of the hypoxic areas, that is, the pimonidazole-positive regions, was observed in tumors treated with HS-1793. The proportions of the hypoxic areas to the entire tumor regions were scored as 19.2% (untreated control) and 14.0% (HS-1793 treated mouse, 1.5 mg/kg), respectively, indicating that the proportion of the hypoxic areas after HS-1793 treatment was significantly decreased compared with that in the untreated control (Fig. 3G).

HS-1793 stimulates anti-angiogenesis through HIF-1α suppression. To examine the effect of HS-1793 on HIF-1α expression in tumor tissue, we performed immunohistochemical analysis of HIF-1α (Fig. 4A). Quantitative data showed that HS-1793 treatment in mice bearing FM3A cells (1.5 mg/kg) affected HIF-1α expression (0.6%) compared with the untreated control (1.9%; Fig. 4B). The mRNA levels of HIF-1α following treatment with HS-1793 were determined on day 30 after treatment. The results showed that HIF-1α mRNA expression decreased significantly after HS-1793 (1.5 mg/kg) treatment compared with that in the untreated control (Fig. 4C).

There are some reports on the anti-angiogenic activity of resveratrol (21). In this study, we examined the anti-angiogenic activity of the resveratrol analog HS-1793 and found that HS-1793 significantly decreased microvessel density (MVD; Fig. 4D). MVD, that is, the percentage of endothelial cells associated with pericytes, is used as a quantitative measure of vascular maturation. Quantitative analysis of pericyte coverage showed 8.29% MVD staining in HS-1793-treated (1.5 mg/kg) FM3A tumors compared with control FM3A tumors (15.68%; Fig. 4E).

The VEGF peptide concentration in mouse serum was significantly higher in untreated control mice (446 pg/ml) than in tumor-free mice (187 pg/ml) but was significantly reduced (P<0.05) in HS-1793-treated mice in a dose-dependent manner (Fig. 4F). Therefore, these findings suggest that HS-1793 inhibits angiogenesis via the downregulation of HIF-1α and VEGF expression under hypoxic conditions of the tumor microenvironment.

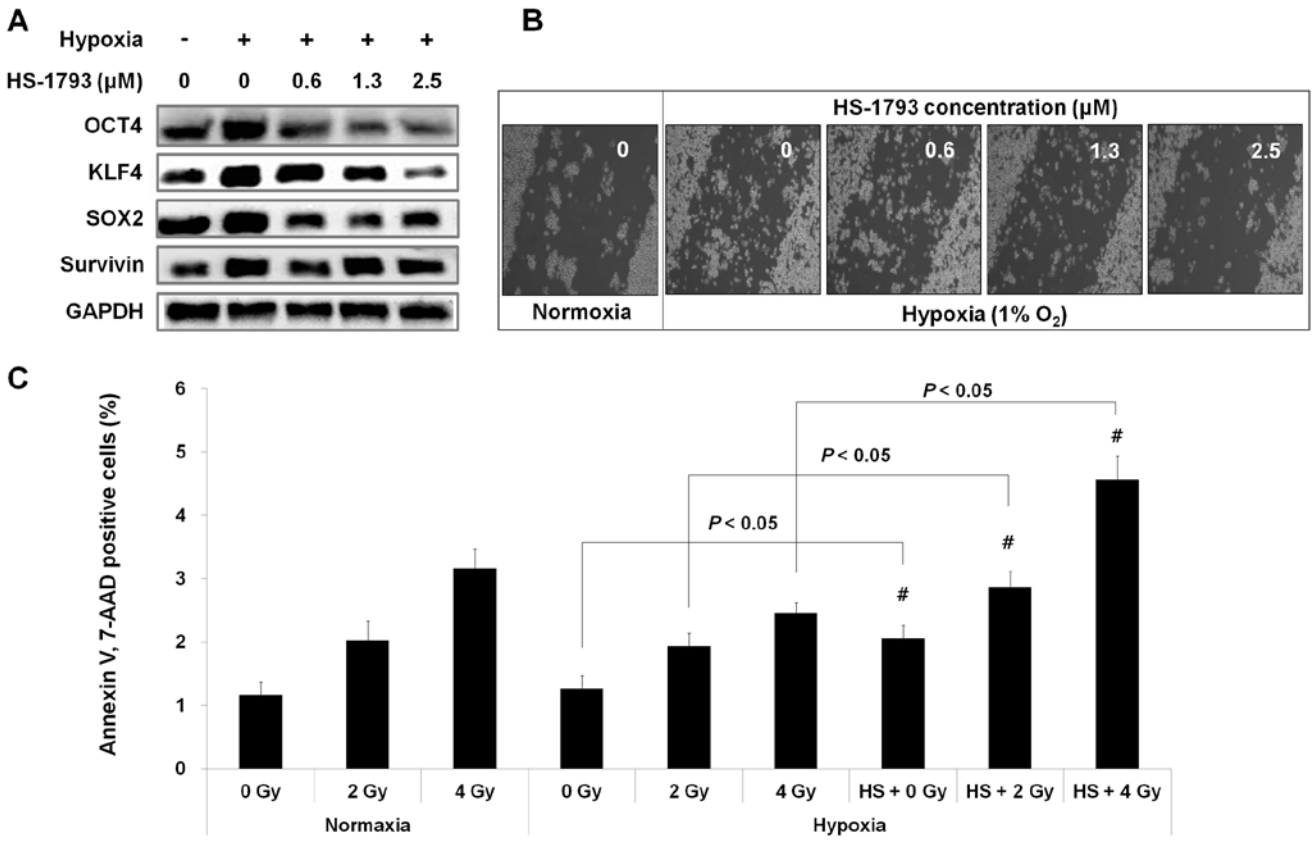

Figure 5. Effect of HS-1793 on hypoxia-induced cancer stem cell characteristics in FM3A cells. The cells were treated with different concentrations of HS-1793 for 2 h. Next, the cells were cultured under normoxic or hypoxic conditions for 12 h. The cell lysates were subjected to immunoblot analysis with anti-OCT4, anti-KLF4, anti-SOX2 and anti-survivin (A). The cells were cultured in normal growth medium to confluence, and then, a scrape in the form of a cross was generated through the confluent monolayer with a plastic pipette tip. The cells were pretreated with vehicle or different concentrations of HS-1793 for 2 h under normoxic or hypoxic conditions. Several wounded areas were marked for orientation, observed and then imaged by phase-contact microscopy 24 h after the scratch (B). Cells were treated with radiation (0, 2 and 4 Gy) or radiation+HS-1793 (2.5 μM). After 72 h, the percentage of Annexin V/PE-positive cells was quantified using flow-assisted cell sorting (C). The data are expressed as the mean ± SD, and significant differences emerged between treated groups by t-test.

To determine the effect of HS-1793 treatment (0.5, 1.0 and 1.5 mg/kg) twice a week for 30 days on tumor growth, changes in the tumor volume were calculated for a period of 30 days following treatment. The tumor volume in the HS-1793-treated mouse group (1.0 and 1.5 mg/kg) was greatly decreased after HS-1793 treatment compared with the untreated control (22). These results indicate that HS-1793 delays tumor growth via the improvement of hypoxia in murine breast cancer.

HS-1793 inhibits hypoxia-induced cancer stem cell properties, including migration and radio-resistance of FM3A cells. Hypoxia increases the number of cells that express CSC markers in bulk populations (23-27). Interestingly, our data showed that HS-1793 decreased the hypoxia induced expression of OCT4, KLF4 and SOX2 protein (Fig. 5A). In other experiments, we investigated the effects of HS-1793 on cell migration under hypoxic conditions. As shown in Fig. 5B, there was minimum migration of FM3A cells under normoxic conditions, while we observed higher levels of FM3A cell migration under hypoxic conditions. However, HS-1793 inhibited hypoxia-induced cell migration in a dose-dependent manner. Accordingly, these results suggest that HS-1793 effectively inhibits the CSC properties of FM3A cells induced by hypoxia. The combinatorial effect of HS-1793 (2.5 μM) and radiation (2 or 4 Gy) in hypoxic FM3A cells was evaluated by the Annexin V/PE apoptosis assay after 12 h of treatment. The 7-AAD-positive cells that also bound Annexin V were defined as late apoptotic cells (Annexin V^+, 7-AAD^+). In Fig. 5C, Annexin V/PE-positive cells were decreased by radiation treatment under hypoxic conditions compared with that under normoxic conditions. However, pretreatment with HS-1793 increased the percentage of late apoptotic cells (4.6±0.38%) compared with the percentage of apoptotic cells in the radiation-treatment (2.5±0.15%) groups at 1% O_2 (hypoxia). These data suggest that the combinatorial treatment of HS-1793 and radiation increases the therapeutic effect in hypoxic FM3A cells.

Discussion

Breast cancer remains a common and frequently fatal disease among women. Generally, the process of tumor progression is characterized by rapid cellular growth accompanied by alterations in the microenvironment of tumor cells (28). Critical changes in the cellular microenvironment occur under hypoxic conditions, where oxygen supply is inadequate (29). Breast carcinomas usually support their growth by stimulating blood vessel development (angiogenesis). Blood flow within these new vessels is often chaotic, causing periods of hypoxia followed by reperfusion.

Aggressive and metastatic cancer phenotypes that are associated with resistance to radiation therapy, chemotherapy, and a poor treatment outcome can be generated as a result of the hypoxic environment within the tumor (30). Hypoxia detected in the central regions of solid tumors is a leading cause of angiogenesis, a fundamental determinant of malignant tumor progression, by activation of angiogenic factors (31). A key factor in this process is HIF-1. The overexpression of HIF-1α protein has been shown in many human cancers and their metastases and is closely associated with a more aggressive tumor phenotype, including an advanced tumor grade, an increased vascularity, increased resistance to chemo/radiotherapies, and tumor progression (32). The most characterized HIF-regulated gene is VEGF, which is involved in regulating endothelial cell proliferation and blood vessel formation in both normal and cancer cells (33). TGF-β1 is involved in blood vessel formation, and one of its oncogenic functions is to promote tumor angiogenesis, which is associated with its ability to induce VEGF expression (34). Hypoxia, TGF-β1 and VEGF are important factors of the tumor microenvironment that regulate cancer progression and metastasis (35). Recently, resveratrol remarkably inhibited hypoxia-induced HIF-1α accumulation and VEGF expression in both human tongue squamous cell carcinomas (SCC-9) and hepatoma (HepG2) cells and dramatically suppressed hypoxia-stimulated invasiveness of SCC-9 cells *in vitro* (36).

The *in vitro* and *in vivo* findings from this study suggest that the resveratrol analog HS-1793 modulates the hypoxic status and perfusion levels in mouse breast cancer FM3A cells. Our data show that HS-1793 decreased HIF-1α and VEGF expression under hypoxic conditions in FM3A cells (Fig. 1). FM3A cells were treated with TGF-β1 under normal and hypoxic conditions, and HIF-1α and VEGF protein levels were markedly increased by TGF-β1. However, pretreatment with HS-1793 reduced HIF-1α and VEGF expression in FM3A cells dose-dependently (Fig. 2). When the tumor grew to a size of ~500 mm^3, to determine the acute injection efficacy of HS-1793, hypoxia markers (pimonidazole/CCI-103F) and perfusion markers (Hoechst 33342/DiOC7) were used to evaluate changes in tumor hypoxia and perfusion. The results indicated a reduced hypoxic status and enhanced perfusion in the tumor mass. To evaluate the therapeutic effect of HS-1793, mouse breast cancer cells (FM3A) in the logarithmic growth phase were inoculated subcutaneously on the right flank of female C3H/He mice, and the effects of intraperitoneal injection of HS-1793 on HIF-1α and VEGF expression, microvessel density, the change in the hypoxic status and perfusion level, and tumor growth were determined after 4 weeks of treatment. The higher level of serum VEGF in tumor-bearing mice was dose-dependently diminished in the HS-1793-treated groups, a result that was in accordance with the result of HIF-1α expression in the tumor tissue. The tumor tissue of the HS-1793-treated group showed weak expression in immunofluorescent staining of pimonidazole, which specifically binds to thiol-containing proteins in hypoxic cells, and immunohistochemical staining of the endothelial cell marker CD31. However, Hoechst 33342-labeled cells, which represent the blood perfusion of tumor tissue, were markedly increased in the HS-1793-treated groups (Figs. 3 and 4). Finally, HS-1793 delays tumor growth via the improvement of hypoxia in murine breast cancer (22).

CSCs account for a minor fraction of tumor populations; however, those cells might be particularly involved in tumor initiation, proliferation, or metastatic process. HIF-1 has been implicated in the maintenance of CSCs (37,38), and knockdown experiments have concluded that HIFs are required for CSC survival and tumor progression (39). In this study, HS-1793 effectively inhibited hypoxia-induced CSC properties, including the migration of tumor cells under hypoxic conditions in FM3A cells (Fig. 5A and B). Radiation therapy is an effective modality for the treatment of many tumors (40). However, the dose-limiting normal tissue toxicity and radioresistant tumors are still linked to life-threatening radiation treatment failure (41). The enhanced level of HIFs in tumors can be correlated with the level of oxygen within the tumor and has been shown to correlate with tumor radiation resistance (42,43). IR-induced apoptosis was suppressed under hypoxic conditions compared with that under normoxic conditions. However, HS-1793 enhanced IR-induced apoptosis in hypoxic FM3A cells (Fig. 5C).

In conclusion, this study demonstrated that the resveratrol analog HS-1793 exerts anti-metastatic effects by the inhibition of cell migration via the reduction of HIF-1α and VEGF expression, and HS-1793 inhibits hypoxia-induced cancer stem cell properties and enhances IR-induced apoptosis in hypoxic mouse breast tumor FM3A cells. The results of this study demonstrate that HS-1793 increases the therapeutic efficacy of radiation in hypoxic cells through the modulation of the hypoxic condition.

Acknowledgements

This study was supported by the National Research Foundation of Korea (DIRAMS) grant funded by the Korea government (MSIP) (50590-2016) and the [Basic Science Research Program] through the National Research Foundation of Korea (NRF) (NRF-2013 M2A2A 7043665) funded by the Ministry of Science, ICT & Future Planning.

References

1. Keith B and Simon MC: Hypoxia-inducible factors, stem cells, and cancer. Cell 129: 465-472, 2007.
2. Harris AL: Hypoxia - a key regulatory factor in tumour growth. Nat Rev Cancer 2: 38-47, 2002.
3. Folkman J: Angiogenesis in cancer, vascular, rheumatoid and other disease. Nat Med 1: 27-31, 1995.
4. Rich J, Borton A and Wang X: Transforming growth factor-beta signaling in cancer. Microsc Res Tech 52: 363-373, 2001.
5. Sánchez-Elsner T, Botella LM, Velasco B, Corbí A, Attisano L and Bernabéu C: Synergistic cooperation between hypoxia and transforming growth factor-beta pathways on human vascular endothelial growth factor gene expression. J Biol Chem 276: 38527-38535, 2001.
6. Reya T, Morrison SJ, Clarke MF and Weissman IL: Stem cells, cancer, and cancer stem cells. Nature 414: 105-111, 2001.
7. Boyer LA, Lee TI, Cole MF, Johnstone SE, Levine SS, Zucker JP, Guenther MG, Kumar RM, Murray HL, Jenner RG, *et al*: Core transcriptional regulatory circuitry in human embryonic stem cells. Cell 122: 947-956, 2005.
8. Yu F, Li J, Chen H, Fu J, Ray S, Huang S, Zheng H and Ai W: Kruppel-like factor 4 (KLF4) is required for maintenance of breast cancer stem cells and for cell migration and invasion. Oncogene 30: 2161-2172, 2011.
9. Baumann M, Krause M and Hill R: Exploring the role of cancer stem cells in radioresistance. Nat Rev Cancer 8: 545-554, 2008.
10. Jemal A, Siegel R, Ward E, Hao Y, Xu J, Murray T and Thun MJ: Cancer statistics, 2008. CA Cancer J Clin 58: 71-96, 2008.

11. DeSantis C, Siegel R and Jemal A: Breast cancer facts and figures 2007-2008. Amer Can Soc 1-32, 2008.
12. Limer JL and Speirs V: Phyto-oestrogens and breast cancer chemoprevention. Breast Cancer Res 6: 119-127, 2004.
13. Privat C, Telo JP, Bernardes-Genisson V, Vieira A, Souchard JP and Nepveu F: Antioxidant properties of *trans*-epsilon-viniferin as compared to stilbene derivatives in aqueous and nonaqueous media. J Agric Food Chem 50: 1213-1217, 2002.
14. Kong AN, Yu R, Hebbar V, Chen C, Owuor E, Hu R, Ee R and Mandlekar S: Signal transduction events elicited by cancer prevention compounds. Mutat Res 480-481: 231-241, 2001.
15. Jeong SH, Jo WS, Song S, Suh H, Seol SY, Leem SH, Kwon TK and Yoo YH: A novel resveratrol derivative, HS1793, overcomes the resistance conferred by Bcl-2 in human leukemic U937 cells. Biochem Pharmacol 77: 1337-1347, 2009.
16. Raleigh JA, Miller GG, Franko AJ, Koch CJ, Fuciarelli AF and Kelly DA: Fluorescence immunohistochemical detection of hypoxic cells in spheroids and tumours. Br J Cancer 56: 395-400, 1987.
17. Rijken PF, Bernsen HJ, Peters JP, Hodgkiss RJ, Raleigh JA and van der Kogel AJ: Spatial relationship between hypoxia and the (perfused) vascular network in a human glioma xenograft: A quantitative multi-parameter analysis. Int J Radiat Oncol Biol Phys 48: 571-582, 2000.
18. Raleigh JA, Franko AJ, Treiber EO, Lunt JA and Allen PS: Covalent binding of a fluorinated 2-nitroimidazole to EMT-6 tumors in Balb/C mice: Detection by F-19 nuclear magnetic resonance at 2.35 T. Int J Radiat Oncol Biol Phys 12: 1243-1245, 1986.
19. Bernsen HJ, Rijken PF, Hagemeier NE and van der Kogel AJ: A quantitative analysis of vascularization and perfusion of human glioma xenografts at different implantation sites. Microvasc Res 57: 244-257, 1999.
20. Durand RE and Raleigh JA: Identification of nonproliferating but viable hypoxic tumor cells in vivo. Cancer Res 58: 3547-3550, 1998.
21. Garvin S, Ollinger K and Dabrosin C: Resveratrol induces apoptosis and inhibits angiogenesis in human breast cancer xenografts in vivo. Cancer Lett 231: 113-122, 2006.
22. Jeong MH, Yang KM, Choi YJ, Kim SD, Yoo YH, Seo SY, Lee SH, Ryu SR, Lee CM, Suh H, *et al*: Resveratrol analog, HS-1793 enhance anti-tumor immunity by reducing the $CD4^+CD25^+$ regulatory T cells in FM3A tumor bearing mice. Int Immunopharmacol 14: 328-333, 2012.
23. Jögi A, Øra I, Nilsson H, Lindeheim A, Makino Y, Poellinger L, Axelson H and Påhlman S: Hypoxia alters gene expression in human neuroblastoma cells toward an immature and neural crest-like phenotype. Proc Natl Acad Sci USA 99: 7021-7026, 2002.
24. Tavaluc RT, Hart LS, Dicker DT and El-Deiry WS: Effects of low confluency, serum starvation and hypoxia on the side population of cancer cell lines. Cell Cycle 6: 2554-2562, 2007.
25. Giuntoli S, Rovida E, Gozzini A, Barbetti V, Cipolleschi MG, Olivotto M and Dello Sbarba P: Severe hypoxia defines heterogeneity and selects highly immature progenitors within clonal erythroleukemia cells. Stem Cells 25: 1119-1125, 2007.
26. Das B, Tsuchida R, Malkin D, Koren G, Baruchel S and Yeger H: Hypoxia enhances tumor stemness by increasing the invasive and tumorigenic side population fraction. Stem Cells 26: 1818-1830, 2008.
27. McCord AM, Jamal M, Shankavaram UT, Lang FF, Camphausen K and Tofilon PJ: Physiologic oxygen concentration enhances the stem-like properties of $CD133^+$ human glioblastoma cells in vitro. Mol Cancer Res 7: 489-497, 2009.
28. Vaupel P: The role of hypoxia-induced factors in tumor progression. Oncologist 9 (Suppl 5): 10-17, 2004.
29. Ryan HE, Poloni M, McNulty W, Elson D, Gassmann M, Arbeit JM and Johnson RS: Hypoxia-inducible factor-1alpha is a positive factor in solid tumor growth. Cancer Res 60: 4010-4015, 2000.
30. Brizel DM, Scully SP, Harrelson JM, Layfield LJ, Bean JM, Prosnitz LR and Dewhirst MW: Tumor oxygenation predicts for the likelihood of distant metastases in human soft tissue sarcoma. Cancer Res 56: 941-943, 1996.
31. Bergers G and Benjamin LE: Tumorigenesis and the angiogenic switch. Nat Rev Cancer 3: 401-410, 2003.
32. Zagzag D, Zhong H, Scalzitti JM, Laughner E, Simons JW and Semenza GL: Expression of hypoxia-inducible factor 1alpha in brain tumors: Association with angiogenesis, invasion, and progression. Cancer 88: 2606-2618, 2000.
33. Brown NS, Jones A, Fujiyama C, Harris AL and Bicknell R: Thymidine phosphorylase induces carcinoma cell oxidative stress and promotes secretion of angiogenic factors. Cancer Res 60: 6298-6302, 2000.
34. Benckert C, Jonas S, Cramer T, Von Marschall Z, Schäfer G, Peters M, Wagner K, Radke C, Wiedenmann B, Neuhaus P, *et al*: Transforming growth factor beta 1 stimulates vascular endothelial growth factor gene transcription in human cholangiocellular carcinoma cells. Cancer Res 63: 1083-1092, 2003.
35. Ferrara N, Gerber HP and LeCouter J: The biology of VEGF and its receptors. Nat Med 9: 669-676, 2003.
36. Zhang Q, Tang X, Lu QY, Zhang ZF, Brown J and Le AD: Resveratrol inhibits hypoxia-induced accumulation of hypoxia-inducible factor-1alpha and VEGF expression in human tongue squamous cell carcinoma and hepatoma cells. Mol Cancer Ther 4: 1465-1474, 2005.
37. Conley SJ, Gheordunescu E, Kakarala P, Newman B, Korkaya H, Heath AN, Clouthier SG and Wicha MS: Antiangiogenic agents increase breast cancer stem cells via the generation of tumor hypoxia. Proc Natl Acad Sci USA 109: 2784-2789, 2012.
38. Schwab LP, Peacock DL, Majumdar D, Ingels JF, Jensen LC, Smith KD, Cushing RC and Seagroves TN: Hypoxia-inducible factor 1α promotes primary tumor growth and tumor-initiating cell activity in breast cancer. Breast Cancer Res 14: R6, 2012.
39. Li Z, Bao S, Wu Q, Wang H, Eyler C, Sathornsumetee S, Shi Q, Cao Y, Lathia J, McLendon RE, *et al*: Hypoxia-inducible factors regulate tumorigenic capacity of glioma stem cells. Cancer Cell 15: 501-513, 2009.
40. Rosen EM, Fan S, Rockwell S and Goldberg ID: The molecular and cellular basis of radiosensitivity: Implications for understanding how normal tissues and tumors respond to therapeutic radiation. Cancer Invest 17: 56-72, 1999.
41. Camphausen K and Tofilon PJ: Combining radiation and molecular targeting in cancer therapy. Cancer Biol Ther 3: 247-250, 2004.
42. Moeller BJ, Cao Y, Li CY and Dewhirst MW: Radiation activates HIF-1 to regulate vascular radiosensitivity in tumors: Role of reoxygenation, free radicals, and stress granules. Cancer Cell 5: 429-441, 2004.
43. Dewhirst MW, Cao Y and Moeller B: Cycling hypoxia and free radicals regulate angiogenesis and radiotherapy response. Nat Rev Cancer 8: 425-437, 2008.